This article has been accepted for publication in a future issue of this journal, but has not been fully edited. Content may change prior to final publication. Citation information: DOI10.1109/TBC.2012.2207249, IEEE Transactions on Broadcasting

Implementation and Co-Simulation of Hybrid Pilot-Aided Channel Estimation With Decision Feedback Equalizer for OFDM Systems

Wei Li, Yue Zhang, Li-Ke Huang, Carsten Maple, and John Cosmas

***Abstract*—This paper introduces novel hybrid pilot-aided channel estimation with decision feedback equalizer(DFE) for OFDM systems and its corresponding hardware co-simulation platform. This pilot-aided channel estimation algorithm consists of two parts: coarse estimation and fine estimation. In the coarse estimation, the combined classical channel estimation methods including carrier frequency offset (CFO) and channel impulse response (CIR) estimation are used. Based on the received training sequence and pilot tones in the frequency domain, the major CFO, sampling clock frequency offset (SFO) and CIR effect coefficients are derived. In the fine estimation, the pilot-aided polynomial interpolation estimation combined with a new decision feedback equalizer scheme based on minimum mean squared error (MMSE) criteria is proposed to reduce the residual effect caused by imperfect CIR equalizer, SFO and CFO. At the same time, for the purpose of speeding up the whole development and verification process, a new architecture of co-simulation platform which combines software and hardware is introduced. The simulation results on the co-simulation platform indicate that the proposed hybrid channel estimation scheme can enhance the receiver performance by 6 dB in terms of error vector magnitude (EVM) over large ranges of CFO and SFO and BER performance by 7 dB for SNR range over 15 dB.**

***Index Terms*—CFO, channel estimation, co-simulation, DFE, EVM, FPGA, MMSE, OFDM, SFO.**

I. Introduction

As A mature and well-established technology for wireless communication, the Orthogonal Frequency Division Multiplex (OFDM) scheme [1] has been adopted for various standards, including the 802.11agn wireless LAN and digital video broadcasting (DVB) systems. The major advantage of OFDM system is that it makes efficient use of the spectrum by allowing overlap and is more resistant to frequency selective fading than single carrier systems. The disadvantage is that it is more sensitive to carrier frequency offset and drift. The received OFDM signal is sensitive the carrier frequency offset, sampling frequency offset and frequency selective fading channel [1]. Therefore, it is necessary to develop hybrid synchronization and channel estimation algorithm to improve the error performance and channel capacity in the OFDM system especially for the high order QAM modulation.

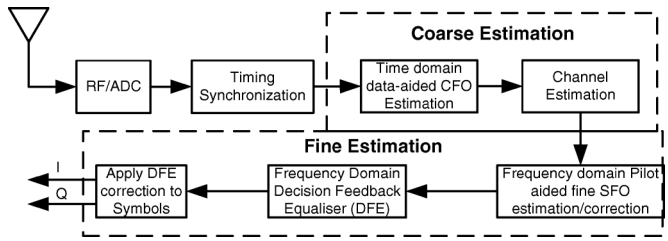

Fig. 1. System diagram for hybrid pilot-aided channel estimation.

Large amount of investigation have been conducted on OFDM systems. The compensation of CFO has been studied in works of [2]–[4], which propose both frequency and time domain estimation algorithms. The channel estimation algorithm [5], [6] introduce blind estimation approaches which is a relatively complex structure, while [7], [8] investigate data-aided channel estimation methods which exhibits good performance. Most of the algorithms on SFO estimation is based on pilot-aid methods or training sequence [9], [10]. The least mean-square (LMS) error adaptive equalization scheme is presented by Widrow and Hoff [11]. Two main structures are developed: linear equalizer and nonlinear equalizer. In [12], [13], the zero forcing (ZF) and MMSE criteria are introduced. In [14], the performance of matched filter (MF), least squares (LS), and MMSE equalizer have been investigated. Furthermore, in [15]–[17], the joint estimation without DFE structure is investigated and gives a better performance. However, it is expected that a hybrid channel estimation algorithm with DFE structure will enhance the EVM performance.

The objective of this paper is to develop synchronization and hybrid pilot-aided channel estimation algorithm with decision feedback equalizer which is easy to be implemented for OFDM system as shown in Fig. 1 and build a hardware co-simulation

Manuscript received March 21, 2012; revised June 15, 2012; accepted June 21, 2012.

W. Li is with the Institute for Research in Applicable Computing, University of Bedfordshire, Luton, LU1 3JU, U.K. (e-mail: Wei.Li@beds.ac.uk).

Y. Zhang is with the Department of Computer Science and Technology, University of Bedfordshrie, Luton LU1 3JU, U.K. (e-mail: Yue_zhang@ieee.org).

L.-K. Huang is Aeroflex, Stevenage SG1 2AN, U.K. (e-mail: like.huang@gmail.com).

C. Maple is the University of Bedfordshire, Luton LU1 3JU, UK (e-mail: Carsten.Maple@beds.ac.uk).

J. Cosmas is with the School of Engineering and Design Brunel University, London UB8 3PH, UK. (e-mail: John.Cosmas@Brunel.ac.uk).

Color versions of one or more of the figures in this paper are available online at http://ieeexplore.ieee.org.

Digital Object Identifier 10.1109/TBC.2012.2207249

This article has been accepted for publication in a future issue of this journal, but has not been fully edited. Content may change prior to final publication. Citation information: DOI10.1109/TBC.2012.2207249, IEEE Transactions on Broadcasting

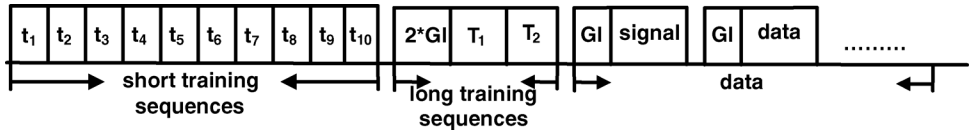

Fig. 2. Training sequences for OFDM systems.

platform for performance verification (see Fig. 2). To achieve high performance, the algorithm adopts the similar scheme as [16] proposed. Due to its high complexity, the algorithm is hard to implement in hardware such as FPGA and DSP which mostly conduct linear mathematical operation whereas the algorithm in [16] makes use of non-linear derivation. To reduce the computation complexity, this algorithm makes full use of some classical algorithms and combines these algorithms with novel DFE. Compared with the previous single types of channel estimation, this algorithm shows high performance and low computation complexity.

This algorithm scheme consists of coarse timing synchronization and hybrid channel estimation based on coarse estimation and fine estimation in both time domain and frequency domain. Firstly, in coarse estimation, the hybrid algorithm makes full use of the long and short training sequences and utilizes the correlation between two adjacent continuous training sequences. This process can suppress dominant ICI effects introduced by CFO in time domain. Then, a frequency domain least square (LS) CIR estimation [18] is presented to compensate for the corruption of the frequency selective channel. Afterwards, a frequency domain estimation based on received signal containing pilot tones is carried out to suppress the sampling frequency offset and residual carrier frequency offset. The polynomial interpolation method is used to refine fine estimation for residual CFO, SFO and CIR effect. With the previous classical hybrid methods, the estimation results show a relatively good performance whilst still remaining a little rotation on the constellation. Therefore, to recover the transmitted constellation, an equalizer is essential for the fine channel estimation to overcome the residual CFO, SFO and CIR effect.

For the investigation of DFE, we consider an approach to minimum mean square error (MMSE)-based equalization that enables significant reduction in rotation of constellation without using the training sequences or pilots. The novel scheme makes full use of received data point by using the same approach of averaging the received signal in linear equalizer. In other words, this DFE scheme first assumes the equalizer is a linear estimator which can be derived out the parameters which will be used in the later optimization. All the parameters are optimized under the criteria of MMSE including the forward filter and feedback filter in the DFE structure. Without loss of generality, OFDM system selected for simulation is based on 801.11agn wireless LAN.

As the prototype algorithm developed in MATLAB does not take the reliability and hardware consumption into account, it is necessary to verify the robustness and performance in both software and hardware environments which is known as co-simulation. There exist numbers of techniques for hardware-software co-simulation. Factors including performance, timing accuracy and speed affect the choice for different co-simulation structures [19]–[21]. Simulation which is created from a combined virtual hardware environment that is combined with the software provides the fastest development process and the fastest interface between the hardware and software. However, this method lacks the accuracy of the CPU instruction period [19]. Hence, a co-simulation platform containing high performance FPGAs and an interface communication mechanism between the software and hardware which can verify various wireless communication algorithms is developed. The experiment and results from this hardware co-simulation platform show that this hybrid pilot-aided channel estimation with DFE can achieve relatively high performance on frequency offset and channel estimation with 6 dB enhancement in terms of EVM. The whole hybrid algorithm is robust while evaluated on the co-simulation platform.

The rest of the paper is organized as follows: The OFDM system is described in Section II. In Section III, the coarse estimation algorithm is introduced. The fine estimation with DFE scheme is described in Section IV. Section V shows the co-simulation platform and the development flow. Section VI shows the design of co-simulation. Section VII shows the simulation results for the hybrid channel estimation with DFE presented and the performance of the co-simulation platform.

II. System Model

This section describes the OFDM system model. The ICI effects caused by CFO and SFO will be discussed. In addition, the signal deterioration caused by the channel distortion is also presented.

A. OFDM System Model

OFDM is a promising technique for achieving high data rate and combating multipath fading in wireless communication. OFDM can be thought of as a hybrid of multi-carrier modulation (MCM) and frequency shift keying (FSK) modulation. Orthogonality among the carriers is achieved by separating the carriers by an integer multiple of the inverse of symbol duration of the parallel bit streams.

The system has N subcarriers and therefore uses an IFFT of size N for modulation. Firstly, the input serial data, in the form of BPSK, QPSK, or 64-QAM sub-symbols, is converted to parallel data $X_m(K) \in A\{A_l, l = 0, \ldots, M-1\}$ where A is the M-ary modulation signaling set, and m is the OFDM symbol with k representing the OFDM sub-carrier indices. Suppose the sample period is T and the IFFT size is N and $X_l(k)$ is the data in kth sub carrier of the lth symbol. In order to avoid inter-symbol interference (ISI) due to channel delay spread, the OFDM symbol is inserted with a guard interval of length N_g.

This article has been accepted for publication in a future issue of this journal, but has not been fully edited. Content may change prior to final publication. Citation information: DOI10.1109/TBC.2012.2207249, IEEE Transactions on Broadcasting

Thus, the length of one OFDM symbol is $N + N_g$, the transmitted complex signal can be described as [1]:

$$s(t) = \frac{1}{N} \sum_{l=-\infty}^{+\infty} \sum_{k=-\frac{k}{2}}^{\frac{K}{2}-1} X_l(k) e^{\frac{j2\pi k}{NT}(t-T_g-lT_s)} \bullet u(t-lT) \quad (1)$$

where $T_g = N_g T$ is the guard interval length and T_s is OFDM symbol length after inserting CP.

The OFDM signal is transmitted over a frequency selective fading channel

$$h(t) = \sum_{i=0}^{L-1} h_i(t)\delta(n-\tau_i) \quad (2)$$

where $h_i(t)$ is complex gain for ith channel and τ_i is the delay for ith channel. We assume that the taps of channel is uncorrelated and τ_i is a constant. We get the sampled received signal:

$$r_{l,k} = sum_i h_i(kT) \bullet s(kT-\tau_i) + n(kT) \quad (3)$$

where $n(kT)$ is the additive white Gaussian noise, which has zero mean and variance of σ^2.

B. Timing Offset Model

Since the receivers are not able to know the time scale of transmitted signal beforehand, the start position of the received signal may deviate from ideal setting by a time ε. As a result, this deviation staggers the receiver's FFT-window away from received OFDM symbol.

Assuming that the time deviate is $\varepsilon = k_\varepsilon T$ and N_g is the number of sample point of the guard interval and N_s is the number of is OFDM symbol length after inserting CP, the receiver time scale in terms of sample points is:

$$k' = k + k_\varepsilon + N_g + l \bullet N_s \quad (4)$$

Then the received signal can be expressed as:

$$\mathrm{r}_{l,k} = \sum_i h_i(t) \bullet s(k'T-\tau_i) + n(k'T) \quad (5)$$

Due to the time offset, some portions of the ideal channel are shifted outside the channel estimation window. The part which shifts outside estimation window is useless for channel estimation $W(t)$ and may cause an additional noise whose variance is [1]:

$$\sigma_{add}^2 = E\left|\tilde{H}_{l,k}^{n_\varepsilon} - H_{l,k}^{\varepsilon}\right|^2 = \frac{K}{N}\sum_i |h_i|^2 \left|1 - W(\tau_i - \varepsilon T)\right|^2 \quad (6)$$

The above formula indicates that the noise variance is sensitive to the accuracy of channel estimation. Therefore, the time synchronization must be carried out.

C. CFO and SFO System Model

However, the frequency difference between transmitter and receiver and the Doppler shift can cause the CFO of Δf in the received signal. Furthermore, the sample period will be non-ideal T', which will cause SFO. The above affects will cause the ICI and greatly degrade the Frequency Domain (FD) estimation performance. We introduce the SFO term $\eta = (\Delta T/T)$, $\Delta T = T' - T$, CFO term $\varepsilon = \Delta f N T = (\Delta f/f)(NTf)$ and $\varepsilon_\eta = (1+\eta)\varepsilon$. Equation (3) is modified to [1]:

$$r_{l,k} = \frac{e^{j\frac{2\pi}{N}(N_l+N)\varepsilon_\eta}}{N} \sum_{k=-\frac{K}{2}}^{\frac{K}{2}-1} X_l(k)H(k)e^{j\frac{2\pi}{N}k(1+\eta)} \bullet e^{j\frac{2\pi}{N}\eta N_l} + n_l(n+N_l) \quad (7)$$

where n is the nth data of the lth OFDM symbol and $N_l = N_g + l(N+N_g)$ is the length of received signal. The CFO and SFO term introduces rotations in time domain, which will cause inter carrier interference (ICI) in frequency domain. To suppress ICI, the effect of CFO and SFO in both time domain (TD) and frequency domain (FD) need to be compensated.

III. Synchronization and Coarse Estimation

This section introduces the timing synchronization and coarse estimation, which can preliminary remove the time offset and frequency offset. Firstly, the timing synchronization, which is based on the training sequence, is carried out. Secondly, the classical hybrid estimation of CFO, SFO and CIR based on the continuous training sequence is proposed in the time domain. Then, in the frequency domain, the hybrid estimation of CFO and SFO is based on the scattered pilot tones. The synchronization and coarse estimation algorithm is elaborated choused to reduce the whole complexity joint algorithm. The system diagram is shown in Fig. 1

A. Timing Synchronization

As described in Section I, the estimation window must be aligned correctly with the received signal, which indicates that time offset should be estimated accurately. Delay and correlation algorithm [30] relatively has a high performance and low computation complexity which is easy to be realized. To simplify the whole structure of the joint algorithm, we adopt delay and correlation algorithm. In this algorithm, two sliding windows are constructed. The window c is a cross-correlation between the received signal and a delayed version of the received signal, whilst window p represents the received signal energy during the cross-correlation window [22].

$$m_n = \frac{|c_n|^2}{(p_n)^2} = \frac{\sum_{k=0}^{L-1} r_{n+k} r_{n+k+D}^*}{\sum_{k=0}^{L-1} |r_{n+k+D}|^2} \quad (8)$$

Two sliding windows are constructed. The window c is a cross-correlation between the received signal and a delayed version of the received signal, whilst window p represents the received signal energy during the cross-correlation window. The cross-correlation term c_n sharply rises when the preamble is received thereby causing a quick jump of m_n. This indicates the start of the OFDM packet.

This article has been accepted for publication in a future issue of this journal, but has not been fully edited. Content may change prior to final publication. Citation information: DOI10.1109/TBC.2012.2207249, IEEE Transactions on Broadcasting

B. Carrier Frequency Offset Estimation

Since the subcarrier spacing is narrower than single carrier systems, the slight carrier offset can seriously affect the orthogonality of the subcarrier. It is crucial for OFDM systems to estimate the CFO. The CFO introduces rotations in the time domain, which will greatly degrade the FD estimation performance. Therefore the CFO compensation should be conducted before the CIR, SFO estimation and DFE equalization in frequency domain.

In [24], maximum likelihood (ML) algorithm can significantly improve the performance by exploits the full correlation between any two repetition preamble patterns. Assume the length of the training sequence is L, and the training sequence starts with the ith index in the OFDM symbol. Let $\hat{r}_{l,i}$ be the corrupted signal and $r_{l,i}$ be ideal signal. The correlation is formed as below [22]:

$$\begin{aligned} E\{\hat{S}_L\} &= E\left\{\sum_{k=0}^{L-1} \hat{r}_{l,k} \bullet \hat{r}^*_{l,k+L}\right\} \\ &= e^{j\frac{2\pi}{N}L\varepsilon} \sum_{i=0}^{L-1} r_{l,k} \bullet r^*_{l,k+L} \\ &= e^{j\frac{2\pi}{N}L\varepsilon} \bullet S_L \end{aligned} \tag{9}$$

Taking the angle of $E(\hat{S}_L)$, we get ε:

$$\varepsilon = \arg\{\hat{S}_L\} \bullet \frac{N}{2\pi \bullet L} \tag{10}$$

As described before, $\varepsilon = \Delta f NT$, the frequency offset will be:

$$\Delta f = \arg\{\hat{S}_L\} \bullet \frac{1}{2\pi \bullet T \bullet L} \tag{11}$$

As depicted in (9) and (11), this carrier frequency offset estimation has every simply structure. This structure is extremely easy to implement in the hardware which is another reason the joint channel algorithm adopt this CFO estimation structure.

C. CIR Estimation

Because of the frequency selective and time variant property of the channel, the CIR estimation is important. In general, channel estimation can be classified into two categories: blind estimation which is carried out without knowing the channel statistics and data-aided estimation, which makes use of some transmission signal such as the pilots or a training sequence. This data-aided estimation is more accurate. LS and MMSE algorithms are two major CIR estimation methods. The MMSE algorithm has a better performance while the complexity is high. The LS algorithm has a much lower computation complexity and can achieve similar performance in the condition of high SNR [24]. When the channel is slow fading and Gaussian, we can estimate the channel by using LS estimation [15]. Let X_k represent training symbols on the kth subcarrier of the OFDM symbol in the frequency domain. After the FFT processing, the received training data can be expressed as:

$$R_{l,k} = H_k X_k + W_k \tag{12}$$

where H_k is the frequency response of channel and $W_{l,.k}$ is additive noise. The aim of LS is to minimize the square error of channel estimation:

$$(Y - X\hat{H})^H (Y - X\hat{H}) \tag{13}$$

In [22], the CIR estimation is calculated using this criterion:

$$\begin{aligned} \hat{H}_k &= \frac{1}{2}(R_{l,k} + R_{2,k})X^*_k \\ &= \frac{1}{2}(H_k X_k + W_{1,k} + H_k X_k + W_{2,k})X^*_k \\ &= H_k + \frac{1}{2}(W_{1,k} + W_{2,k})X^*_k \end{aligned} \tag{14}$$

where the amplitude of training data is normalized. The noise samples are assumed to be statistically independent. According to (14), the CIR estimation is the correlation of input signals R and reference signal X^*_k in frequency domain, therefore the amount of computation is quite small. This CIR estimation method is also easy to implement on the FPGA or DSP hardware.

Thus the frequency selective channel is then compensated. Because the LS algorithm does not take in account the correlation between the channel statistics and the noise, the estimation performance will become worse in low SNR. The accurate compensation is then carried out using fine estimation.

IV. Fine Estimation

Though the timing synchronization and coarse estimation eliminate most of the CFO and the corruption of channel, there may still be a SFO, which seriously affects the performance of systems.

A. Pilot-Aided Polynomial Interpolation Method

With the CFO and CIR compensated, the received signal is corrupted by the SFO. The SFO can cause a rotation on the constellation. As the SFO can cause a time deviation on every sampling point in time domain and a phase rotation on every sampling point in frequency domain, some pilot tones are inserted to correct these phase rotations. A great many of SFO estimation are presented in [25], [26]. This pilot aided fine estimation consists of algorithms to estimate the SFO at pilot frequencies and to linear interpolate the none-pilot tones. Moreover, with the estimated pilot phase rotations, we can calculate out the approximate phase rotation on the other subcarriers by interpolation. The post-FFT signal is [9]:

$$X_{l,k} = \left(e^{j2\pi\phi_k} e^{j2\pi(\frac{lN_s+N_g}{N})\phi_k}\right) \alpha(\phi_k) a_{l,k} H_k + n_{\Omega;l,k} + n_{l,k} \tag{15}$$

with residual frequency offset

$$\phi_k \approx \Delta f NT + \eta \bullet k \tag{16}$$

$$N_s = N + N_g \tag{17}$$

The factor $\alpha(\phi_k)$ represents the attenuation as a result of residual frequency offset, whose variation is so small that it can be neglected. The term $n_{\Omega;l,k}$ stands for ICI noise. The phase rotation is shown in Fig. 3.

This article has been accepted for publication in a future issue of this journal, but has not been fully edited. Content may change prior to final publication. Citation information: DOI10.1109/TBC.2012.2207249, IEEE Transactions on Broadcasting

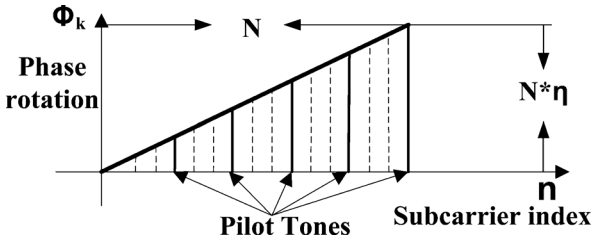

Fig. 3. Phase rotation by residual CFO, SFO, and CIR effect.

Assume the pilot locates on the kth subcarrier; the correlation of two adjacent OFDM symbols yields the phase rotation:

$$z_{l.k} = x_{l,k} \bullet x^*_{l-1,k} = e^{j2\pi\left(\frac{N_s+N_g}{N}\right)} \alpha^2(\phi_k) \left|H_k\right|^2 \beta^2 \sigma^2_\alpha + n_l \tag{18}$$

where σ^2_α is the transmit power of pilot symbol located on the kth subcarrier and β is a constant. According to the above formula, the term $\alpha^2(\phi_k)|H_k|^2\beta^2\sigma^2_\alpha$ is a constant. Therefore the phase rotation can be using the following formula.

The phase rotation on the kth subcarrier between two adjacent OFDM symbols is:

$$\Delta\varphi_k = \frac{1}{2\pi}\measuredangle z_{l,k} = \frac{1}{2\pi} x_{l,k} x^*_{l.k} \tag{19}$$

The phase rotation of the pilot tones can be estimated using the above algorithm, while the phase rotation of the data tones is achieved via interpolation. Several approaches including of polynomial interpolation (linear, second and cubic) have been studied [28]. The linear interpolation has the least computation complexity among the above interpolation methods. Consider the rotation has a linear relationship with the index of data tones and pilot tones. This paper adopts linear interpolation method.

Assume X to be the index of the pilot tones in one OFDM symbol and φ to be the corresponding phase rotation on the pilot tones, then the relationship between can be expressed:

$$\beta_1 + x_{pi}\beta_2 = \varphi_{pi} \tag{20}$$

This can be written in matrix form as:

$$\phi_P = X_P \beta \tag{21}$$

Where $X = \begin{pmatrix} 1 & x_{p1} \\ 1 & x_{p2} \\ \vdots & \vdots \\ 1 & x_{pk} \end{pmatrix}$, and X_{pk} is the pkth pilots index in one OFDM symbol.

The coefficient matrix is $\beta = \binom{\beta_1}{\beta_2}$.

And $\phi_P = \begin{pmatrix} \varphi_{p1} \\ \varphi_{p2} \\ \vdots \\ \varphi_{pk} \end{pmatrix}$ and φ_{pk} is the rotation of pkth pilot tones.

And the estimated coefficient is:

$$\hat{\beta} = \left(X_P^T X_P\right)^{-1} X_P^T \phi_P \tag{22}$$

Accordingly, all the other phase rotations can be calculated:

$$\phi = X\hat{\beta} \tag{23}$$

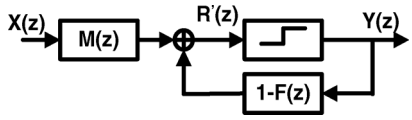

Fig. 4. System diagram for the DFE scheme.

Where

$$\phi = \begin{pmatrix} \varphi_1 \\ \varphi_2 \\ \vdots \\ \varphi_N \end{pmatrix} \text{ and } X = \begin{pmatrix} 1 & x_1 \\ 1 & x_2 \\ \vdots & \vdots \\ 1 & x_N \end{pmatrix}$$

The frequency domain aided SFO estimation algorithm can greatly enhance the received signal's error performance. The phase rotation is eliminated to the great extent.

B. Decision Feedback Equalizer

This decision feedback equalizer is developed to eliminate the residual rotation. With the preceding compensating, the EVM performance of the received signal can be largely improved. However, there are is some rotation on the constellation mainly due to the noise and residual frequency offset. These tiny rotations can be corrected by this proposed DFE.

Two main schemes are developed for error adaptive equalization: linear equalizer and nonlinear equalizer. The linear equalizer aims to minimize mean-square error for time-dispersive additive Gaussian noise channels. However, linear equalizer performance falls over highly dispersive channels due to the limitations of matched filter performance bound. Decision feedback equalizer belongs to nonlinear equalization. Since its reduction in implementation complexity, the DFE receiver structure has drawn considerable attention from many researchers. As shown in Fig. 4, the equalized signal is the sum of the outputs of forward filter and outputs of feedback filter. According to these filters' optimization criteria, DFE is classified into Zero Forcing (ZF) and MMSE structure. The ZF equalizer has a simpler structure which supposes the channel SNR be infinite. However, when the channel is severely frequency selective, this simplification may cause the equalizer not to show the expected functionality. In addition, the ZF criterion neglects the effect of noise, thus it is not so robust to the low SNR scenario. The MMSE-DFE structure presented in this paper adopts a new approach to minimize the mean square error (MSE) for the OFDM systems channel estimation. It takes the noise into account and can enhance the performance of OFDM systems especially when SNR is low.

Let y_k be the output of the equalizer, x_k be input of the equalizer and r'_k be the accumulated result of the feedback filter and forward filter. The corresponding z-transforms are $X(z)Y(z)$, $R'(z)$ as depicted in Fig. 4 [29]. The forward filter is $M(z)$ and feedback filter is $1 - F(z)$. According to the minimum mean square error criteria, the optimization problem is [12]:

$$\min_{W(D),B(D)} E\left[\left|y_k - r'_k\right|^2\right] \tag{24}$$

which implies that to get minimum MSE, optimal feedback filter $1 - F(z)$ and forward filter $M(z)$ is essential. As all the re-

This article has been accepted for publication in a future issue of this journal, but has not been fully edited. Content may change prior to final publication. Citation information: DOI10.1109/TBC.2012.2207249, IEEE Transactions on Broadcasting

ceived data points distribute around ideal constellation points and there is some deviation between the received signal and the ideal constellation points. The deviation was caused by residual noise, CFO, SFO, CIR effects and the receiver implementation distortion with main factors being eliminated by the preceding estimation. The distance between received signal and the nearest ideal constellation point is $d_k = |y_k - r'_k|$. Thus, the optimization problem becomes $\min_{\mathrm{M(D)},\mathrm{F(D)}} \mathrm{E}[\mathrm{d}_\mathrm{k}^2]$, in other words the optimization problem is to find out optimum M (z) and F (z).

Assume the probability of received data points that appears on the constellation is a constant p, and then the term $\mathrm{E}[\mathrm{d}_\mathrm{k}^2]$ is expressed as:

$$E\left[d_k^2\right] = p\sum_{k=1}^{M} d_k^2 \tag{25}$$

where M is the number of received data point. According to the inequality [33]:

$$\frac{\sum_{i=1}^{M} d_i}{M} \leq \sqrt{\frac{\sum_{i=1}^{M} d_i^2}{M}} \tag{26}$$

It reveals that if we average the past M data points which are distributed around the same constellation points then the minimum average $\mathrm{E}[\mathrm{d}_\mathrm{k}^2]$ can be obtained, which indicates a MMSE signal. Therefore, consider a linear feedback filter $1-F(D)$ that averages past M received points to obtain a minimum MSE:

$$\hat{Y}_k = \sum_{m=0}^{M} a_m y_{k-m} = \sum_{m=0}^{M} \frac{1}{M} y_{k-m} \tag{27}$$

The aim of this feedback filter is that it averages a cluster of past M data points which deviate from one of the constellation points and output a data which contains as an average error of these M data. Then, this data is passed back to accumulate with the output of the forward filter and shape the received signal in order to obtain a minimum error. Since the feedback filter $1 - F(z)$ is assumed to be a linear filter as described above, the remaining part of the algorithm is to derive the forward filter $M(z)$.

Definition: The received signal which is corrupted by the frequency selective channel is [29]:

$$\begin{aligned}\hat{y}(t) &= \hat{x}(t) + z(t) \\ &= \sum_{l=0}^{K-1}\sum_{k=0}^{N-1} x_{l,k}\left[\varphi_k(t-lT) \bullet h(t)\right] + n(t)\end{aligned} \tag{28}$$

where $\varphi_k(t-lT)$ is $e^{(j2\pi k/NT)(t-lT)}$ with l standing for the symbol time and k standing for basis coefficient of FFT and $n(t)$ standing for Gaussian noise and T is the sample period.

The terms $\varphi_k(t-lT)$ can be regarded as the basis of the signal space, and each $\varphi_k(t-lT)$ will be modulated by the frequency selective channel with pulse response:

$$p_k(t) = \varphi_k(t) * h(t) \tag{29}$$

The normalized pulse response is:

$$\psi_k(t) = \frac{p_k(t)}{\|p_k\|}$$

Then, define the correlation of the normalized pulse response is:

$$q_l = <\psi_0, \psi_l> = \int \psi(t)\psi^*(t-lT)dt \tag{30}$$

Then, we get the sequence of pulse response $\{q_0, q_1, \ldots q_N\}$. By taking the z-transform, we get $Q(z)$

The average power of received signal is $\varepsilon_X = E[\|x_k\|^2]$.

Derivation: The main optimization target is to minimize MSE or the error $E(D)$:

$$E(z) = Y(z) - R'(z) \tag{31}$$

with the limiting condition (27) and:

$$R'(z) = M(z)X(z) + (1 - F(z))\,Y(z) \tag{32}$$

Simplify (32) obtains:

$$E(z) = F(z)X(z) - M(z)Y(z) \tag{33}$$

In [29], it has been shown that the MMSE of $E[|e_k|^2]$ can be obtained by using orthogonality principle:

$$\begin{aligned}&E\left[E(z)X^*(z^{-*})\right] \\ &\quad = E\left[\left[F(z)Y(z) - M(z)X(z)\right]X^*(z^{-*})\right] = 0\end{aligned} \tag{34}$$

Hence,

$$M_{opt}(z) = \frac{F(z)E\left[Y(z)X^*(z^{-*})\right]}{E\left[X(Z)X^*(z^{-*})\right]} \tag{35}$$

Thus,

$$M_{opt}(z) = \frac{F(z)\varepsilon_x}{\|p\|^2 Q(z)\varepsilon_x + N_0} \tag{36}$$

Hence the equalizer can be expressed as below:

The feedback filter:

$$1 - F(z) = 1 - \sum_{k=0}^{K} \frac{1}{M} z^{-k} \tag{37}$$

The forward filter:

$$M_{opt}(z) = \frac{F(z)\varepsilon_x}{\|p\|^2 Q(z)\varepsilon_x + N_0} \tag{38}$$

As described above, the decision feedback equalizer needs the channel frequency response to shape the input signal. Therefore, this equalizer is adaptive to the channel status. The feedback filter is a FIR filter whose tap coefficients are changed according to average times. The coefficient of forward filter, which can be an IIR or FIR filter, changes according to the channel status and the feedback filter. Obviously, it is easy to implement both filters on the hardware platform.

As for the complexity and performance analysis, according to (37) and (38), the feedback filter can be realized in forms of FIR

This article has been accepted for publication in a future issue of this journal, but has not been fully edited. Content may change prior to final publication. Citation information: DOI10.1109/TBC.2012.2207249, IEEE Transactions on Broadcasting

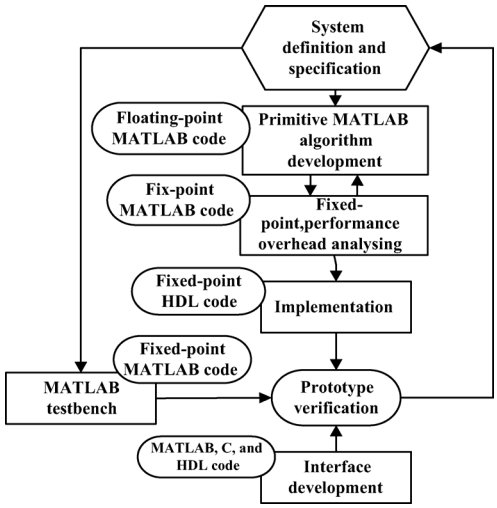

Fig. 5. Co-simulation platform design flow.

filter, which is extremely easy to be implemented in FPGA or DSP hardware. Similarly, the forward filter is an IIR filter with finite length both in denominator and numerator, this kind of structure is extremely easy to implement in the hardware. Suppose the average point is M and the length of the base sequence is L and the forward filter is implemented in forms of direct form I and feedback filter in form of direct form, it will consume about $2^*\mathrm{M}+\mathrm{L}$ multipliers and $2^*\mathrm{M}+\mathrm{L}+2$ adders.

The SNR of MMSE DFE is derived as:

$$\begin{aligned} & SNR_{MMSE-DFE} \\ & = \frac{\varepsilon_x}{\sigma^2_{MMSE-DFE}} \\ & = \varepsilon_x \bullet \|p\|^2/N_0 \\ & \quad \bullet \exp\left[\frac{T}{2\pi}\int_{\frac{-\pi}{T}}^{\frac{\pi}{T}} \ln\left(Q(e^{-j\omega T}) + N_0/\varepsilon_x \bullet \|p\|^2\right) d\omega\right] \\ & = \frac{\varepsilon_x}{S_e(e^{-j\omega T})} \end{aligned} \tag{39}$$

where $S_e(e^{-j\omega T})$ is the power spectral density (PSD) of error sequence caused by the DFE. Accordingly, the channel status and the average power of received signal may have a considerable effect on MMSE SNR. To make full use of this DFE structure, the preceding CIR estimation part should compensate the fading channel well. In time domain, this MMSE DFE is likely to pull the received signal together, and this can reduce the EVM.

V. Co-Simulation Platform Design

This section discusses the design flow on the co-simulation platform. The aim is to verify the algorithm and speed up the development process. Fig. 5 displays the general design process of this co-simulation platform. After the definition of requirements of the communication system, the prototype algorithm is firstly developed in MATLAB. Then, the algorithm is implemented on a hardware platform to verify the performance in a real environment.

Co-simulation platforms such as WARP and OPENAIRINTERFACE [21], allow individual algorithm components to by FPGAs or DSPs and Matlab running simultaneously and exchanging information in a collaborative manner. With the fixed-point simulation platform, this kind of simulation process can verify realizability and evaluate complexity and performance of a dedicated algorithm. The existing co-simulation platforms take considerable amount of time to convert MATLAB code to HDL code. Besides, the hardware-software interface is another important part of co-simulation system. Because algorithm modification may cause re-doing of data interface which may result in data interface development being the most time-consuming step during the whole process system algorithm verification, it is essential to reduce the workload of interface development. Considering that there already exist some tools which can automatically MATLAB code to HDL code, besides the implementation of prototype algorithm, the hardware-software interface is another important part of co-simulation system. Considering all the substructures of the hybrid estimation algorithm such as coarse estimation module, FFT module, CIR estimation module or the DFE module may be verified separately, which means different types of data formats will be transmitted via the interface between the hardware and software. Thus a universal interface that is capable of various throughput and data widths is required. Therefore, the design requirements also include high speed, data transmission stability and compatibility with different data formats for the requirements of different algorithms.

To meet these requirements, a gigabit Ethernet platform was chosen as the interface between MATLAB and FPGA with the maximum data throughput of 1000 M bits/sec. Also, in order to maximum throughput, the extended User Datagram Protocol (UDP) communication protocol was adopted. As described in Fig. 6, the pipeline UDP packet consists of two parts: the payload and header. The header contains an essential check code for the UDP packet and the payload part holds the data which is specified in the header.

The hardware part is the crucial part for the verification. It handles not only the UDP communication between FPGA and PC but also data processing. The hardware is implemented on Xilinx ML605 board with Xilinx Virtex6 FPGA. This co-simulation platform takes advantages of rich on-chip resources of FPGA. The high speed and high performance Digital Clock Management, dedicated MAC Ethernet IP core, LUTs and embedded high speed DSP 48E1 Slice module work collaboratively and provide high speed universal high speed data interface and high performance algorithm realization platform. Fig. 7 form shows the whole hardware consumption, which includes consumption of universal data interface, DFE module. And the consumption of turbo and Viterbi decoder is also listed as a comparison.

The main contribution of this co-simulation is to propose a universal interface between MATLAB and FPGA and to provide a flexible verification platform. It also makes the most of the high speed gigabit Ethernet and the high performance FPGA.

This article has been accepted for publication in a future issue of this journal, but has not been fully edited. Content may change prior to final publication.
Citation information: DOI10.1109/TBC.2012.2207249, IEEE Transactions on Broadcasting

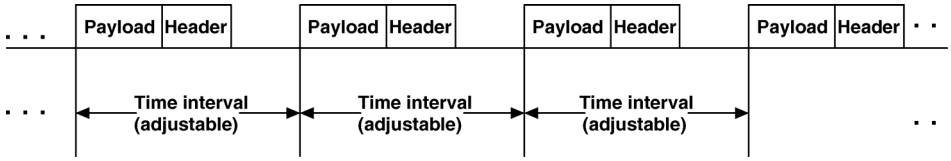

Fig. 6. Transmission of UDP packets.

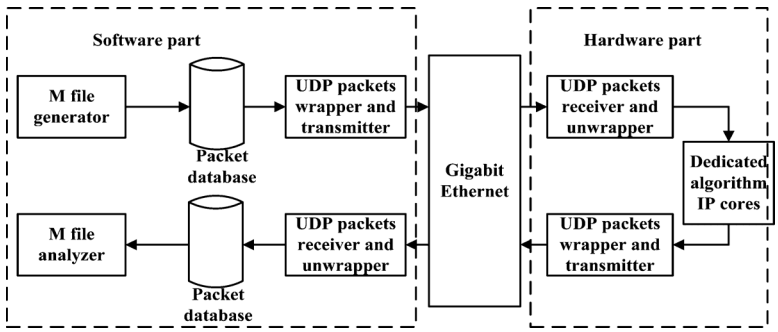

Fig. 7. System diagram of co-simulation platform.

TABLE I
OFDM PARAMETERS

parameter	value
N_{SD}: number of data subcarriers	*48*
N_{SP}: number of pilot subcarriers	*4*
N_{ST}: number of subcarriers, total	*52(N_{SD}+N_{SP})*
T_{FFT}: FFT and IFFT period	*3.2 us*
$P_{PREAMBLE}$: preamble duration	*16 us (T_{SHORT} + T_{LONG})*
T_{SIGNAL}: duration of the signal symbol	*4.0 us (T_{GI} + T_{FFT})*
T_{GI}: GI duration	*0.8 us (T_{FFT}/4)*
$T_{G/2}$: training symbol GI duration	*1.6 us (T_{FFT}/2)*
T_{SYM}: symbol interval	*4 us (T_{GI} + T_{FFT})*

TABLE II
CHANNEL MODELS USED FOR TESTING

Taps	Relative delay (ns)	Fading (dB)
1	0	-4.6
2	15	-2.0
3	25	-3.0
4	50	0
5	150	-4.3
6	225	-6.5
7	400	-3.0
8	525	-15.2
9	750	-21.7

VI. SIMULATION RESULTS

In this section, the performance of this hybrid channel estimation is evaluated via computer simulations. As this hybrid algorithm is a combination of classical algorithm and DFE, the performance of different module is partly simulated. IEEE 802.11n uncoded OFDM system is adopted in this simulation [27]. Table I shows the detail of OFDM symbol. One burst format of data that contains 582 data OFDM frames is used in this simulation. The preamble duration is shown in Fig. 2. In the simulation, we adjust the CFO and SFO by adding an extra carrier frequency offset on the input data to simulate CFO in the real situation and using the FPGA based resampler to change the sample rate of receiver which can bring about a fractional SFO. Then, we consider Rayleigh fading channel with 9 taps for simulation. This mobile channel model is based on an indoor channel model and is described in Table II. In addition, we simulate the Doppler Effect considering the mobile OFDM system.

Fig. 8 shows the MSE curves on the output of CFO estimator under different SNR when SFO is 80 ppm Doppler Effects are not considered in this simulation.

The performance of the system under different carrier frequency offset was compared. Normalized Mean Square Error (NMSE) of the carrier frequency offset estimation is used as the measurement criterion. The NMSE of the carrier frequency

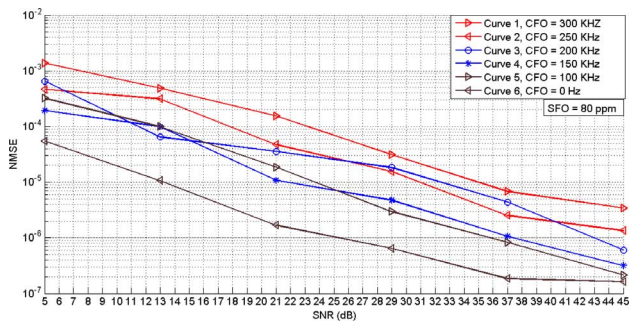

Fig. 8. NMSE of CFO estimation under different SNRs and CFOs.

offset estimates are obtained from 100 Monte Carlo trials on one SNR value and calculated for 50 OFDM symbols.

$$NMSE = \frac{1}{N}\sum_{k=1}^{N}\left(\frac{\Delta f - \Delta\hat{f}(k)}{\Delta f}\right)^2 \qquad (40)$$

where $\Delta\hat{f}(k)$ is the real carrier frequency offset and $\Delta\hat{f}(k)$ is the estimated frequency offset of the kth Monte Carlo run. During the simulations, fewer carrier frequency offsets are chosen which range from 100 kHz to 300 kHz with 50 kHz

This article has been accepted for publication in a future issue of this journal, but has not been fully edited. Content may change prior to final publication. Citation information: DOI10.1109/TBC.2012.2207249, IEEE Transactions on Broadcasting

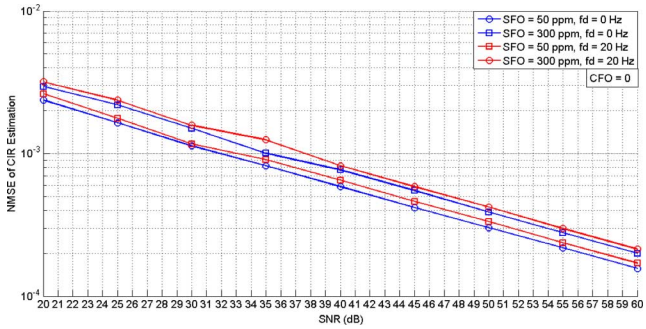

Fig. 9. MSE of CIR estimation for different SFO and Doppler shifts.

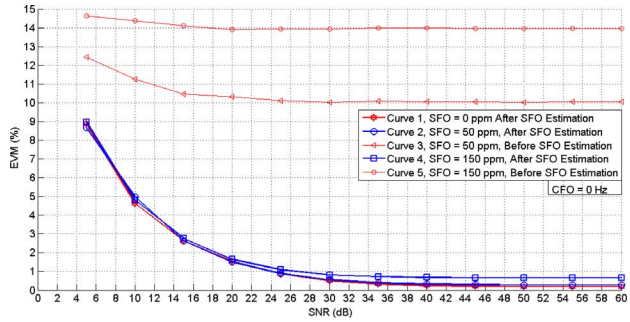

Fig. 10. EVM performance comparison for SFO estimator and preceding parts.

step size. The SNR is defined below which varies from 5 dB to 45 dB.

$$\mathrm{SNR_{dB}} = 10\log_{10}\left(\frac{\mathrm{P_{signal}}}{\mathrm{P_{noise}}}\right) \tag{41}$$

where $\mathrm{P_{signal}}$ is the power of OFDM signal and $\mathrm{P_{noise}}$ is the power of white Gaussian noise.

According to the Fig. 8 the maximum MSE is always below $2 * 10^{-3}$ even when the situation is under the worst SNR of 5 dB, which indicates that estimation is quite accurate. Besides, the MSE for different CFOs are similar with the largest MSE of $1.4{*}10^{-3}$ and smallest of $2.14{*}10^{-7}$ except for the $\mathrm{CFO} = 300$ kHz curve. These curves show that this CFO estimation algorithm is robust to different CFOs and SNRs. The $\mathrm{CFO} = 300$ kHz curve has a higher MSE than the other CFO curves. This is because the subcarrier interval is 312.5 kHz in the adopted OFDM system. When CFO is closed to this value, the value of the subcarriers will be aliased on their adjacent subcarriers, which indicates that the CFO algorithm becomes invalid when CFO extends beyond that value. Thus, $\mathrm{CFO} = 312.5$ kHz becomes a critical frequency, and the estimation for $\mathrm{CFO} = 300$ kHz becomes worse. The MSE keeps relatively low and decreases as SNR increases from 5 dB to 45 dB, which indicates that a higher SNR helps to enhance the estimation performance.

Fig. 9 shows the performance of the CIR estimation method in the indoor channel. This simulation is carried out under different SNR, SFO, Doppler spread scenarios. The NMSE is calculated as depicted in previous simulation. Assume CFO estimation has good performance and the main CFO is eliminated in the CFO estimator with CFO approximately equals 0. Maximum Doppler shifts are set to $\mathrm{f_d} = 0$ Hz and $\mathrm{f_d} = 20$ Hz which respectively correspond to motionless mobile receivers and a mobile receiver with the speed of 2.5 m/s in the indoor environment. Besides, two SFOs are selected to investigate the impact on CIR estimation. As can be seen, the NMSE curves for the two different Doppler frequencies against different SNR are plotted. Generally, the NMSE achieves a good performance with NMSE constantly below 0.3185%, but a higher SNR will lead to a smaller NMSE. There is still fluctuation on the NMSE curve. This is because the square error of CIR estimation $(Y - X\hat{H})^H(Y - X\hat{H})$ in (13) is no longer a least square error under the condition of Rayleigh fading channel which means the LS algorithm is not the optimal for Rayleigh fading channel.

Because the SFO is not compensated in the preceding estimator, SFO has a influence on the CIR estimation. The curves for $\mathrm{SFO} = 300$ ppm are at least $0.3{*}10^{-3}$ higher than the 50 ppm situation in terms of NMSE. As can be seen from Fig. 9, the CIR estimation performance suffers from a slight degradation of 0.01% when Maximum Doppler shift changes from 0 Hz to 20 Hz. This is because Doppler spread inevitably leads to non-constant frequency offset, which can not be compensated in CFO estimator.

Fig. 10 shows the SFO estimation performance for different SFOs and SNRs. The EVM data is calculated from the output signal of SFO estimator as depicted in Fig. 1. As a comparison, the EVM of the received signal before the SFO estimation is also presented. In this simulation, the CFO is still set to 0 kHz and we chose $\mathrm{SFO} = 50$ ppm and $\mathrm{SFO} = 150$ ppm to obtain brief knowledge of the effects of different SFOs. As a reference, the ideal case with perfect synchronization $(\mathrm{SFO} = \mathrm{CFO} = 0)$ is also included in this simulation as Curve 1 depicted. As shown in Fig. 10, Curve 3 and Curve 5 represent the EVM performance before SFO estimation, with a minimum EVM of 4% higher than SFO of estimator processed signal, which shows that SFO has a considerable impact on the preceding estimators. Besides, by comparing Curve 2 with Curve 3, Curve 4 with Curve 5, we can find that the post-SFO-estimation EVM is reduced by as much as 13.3% when SNR equals 60 dB which indicates that the SFO estimator can largely enhance the EVM performance of received signal largely. Though the estimator can improve EVM performance a lot, the residual SFO still have a bit effects on the EVM curve: the EVM for $\mathrm{SFO} = 150$ ppm is about 0.4% higher than that of $\mathrm{SFO} = 50$ ppm after the SFO estimation when SNR is higher than 30 dB as curve 2 and 4 depict. The EVM under lower SNR is still high and needs a further equalization.

Fig. 11 shows the EVM-versus-SNR performance curves under the condition of different SFO which mainly depicts the enhancement brought by DFE. The EVM data are calculated from the output signal of DFE and the pre-DFE part as depicted in Fig. 1. The green curve represents the ideal situation with $\mathrm{CFO} = \mathrm{SFO} = 0$ Hz as a reference. Comparing with the output of pre-DFE part, these EVM values of DFE output are quite low. Comparing the curve 2 and 3, the EVM performance is obviously improved about 1% by DFE when SNR is below 15 dB, and this is mainly due to the average and feedback scheme which use the previous and current received signal to make a prediction. The curve 2 and 4 are close to the ideal

This article has been accepted for publication in a future issue of this journal, but has not been fully edited. Content may change prior to final publication. Citation information: DOI10.1109/TBC.2012.2207249, IEEE Transactions on Broadcasting

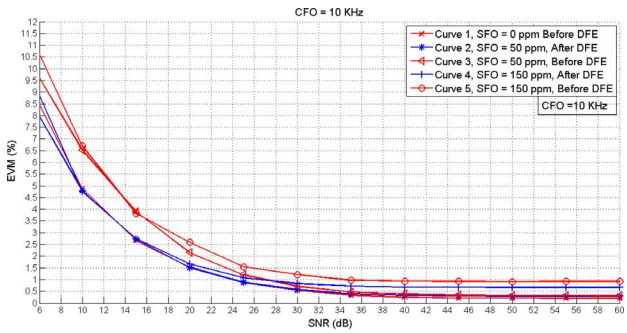

Fig. 11. EVM comparison between DFE and pre-DFE parts.

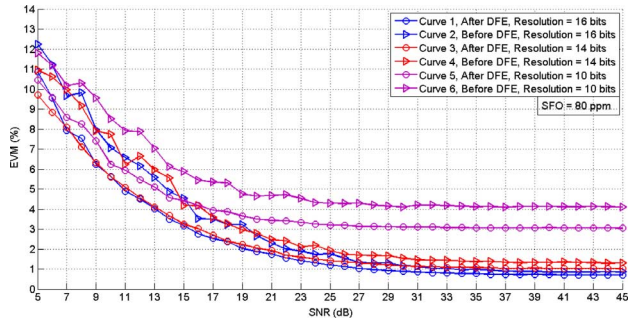

Fig. 12. EVM performance for different data-length on hardware platform.

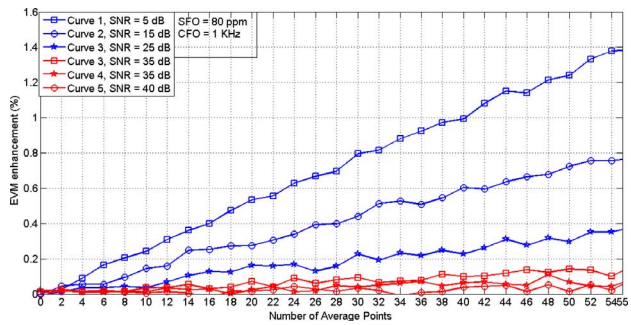

Fig. 13. EVM for different average points.

curve 1 which confirms that this proposed DFE scheme can enhance the performance for different SFOs especially at low SNR. Under the SNR of 25 dB, we find that the EVM can be improved by 6dB at most for the $\mathrm{SFO} = 50$ ppm and 150 ppm after comparing the curve 2 with curve 3; curve 4 with curve 5. As SNR increases, all the curves go remarkably close to the ideal curve and there is still enhancement brought by DFE. This is because the preceding DFE estimators have good performance and the DFE scheme mainly aims to cancel the effect of the noise and residual CFO, SFO and CIR effects by averaging the received signal points.

Fig. 12 shows the EVM-versus-SNR under different word-lengths. The proposed DFE is verified on the FPGA platform with different word-lengths in this simulation In this simulation, 50 data points are averaged in the feedback filter of DFE, that is, $\mathrm{M} = 50$ as depicted in equation (28). The solid Curve 2, 4 and 6 represent the signal EVM after DFE. As a comparison, the EVM before DFE are also plotted in the figure, as depicted by the dotted lines. The blue, red and green lines represent 16, 14 and 12 bits of resolution. Comparing Curve 2, 4 and 6 which represent different resolution, the word length mainly makes a difference when SNR is high. It agrees with the Finite Word-Length Effects theory. Therefore, its effects must be taken into account during implementation. According to Curve 1 and 2, the EVM can be improved by 6 dB at the SNR of 25 dB for the $\mathrm{SFO} = 80$ ppm. The highest EVM degradation observed from curve 2 and 6, as a result of the insufficient size of word length after DFE is 3.00% when SNR is 45 dB. Besides, the DFE is more likely to have effects on the short word length and low SNR scenarios. For example, there is an EVM enhancement of 2.05% when $\mathrm{SNR} = 8$ dB and word-length is 10 bits compared with the EVM before DFE. In other word, the DFE can save two bits word–length to achieve same EVM at 4.1% when SNR is 16 dB. In this case, because of DFE, 10bits-ADC will have the similar EVM performance with 12bits-ADC.

Fig. 13 shows the EVM enhancement versus the number of average points under the different conditions of SNR. The SFO and CFO are set to 80 ppm and 1 kHz. In the lower SNR case, the EVM enhancement is much larger. At the SNR of 5 dB, the DFE gives an enhancement of 2.25% after averaging 100 times while the DFE only gives less than 0.5% enhancement for SNR equals 35 dB. As average numbers grow larger, the enhancement of EVM becomes better and has a linear growth. This is because the DFE structure can make use of more received data points to calculate out the constellation rotation. From Fig. 13, it can be seen that there is a linear relationship between the EVM enhancement versus and the number of average points. Thus, a linear model can be derived out to describe this relation of the performance between the EVM performance and number of average points.

Fig. 14 shows the BER-versus-SNR performance curves in Rayleigh fading channels with sample clock frequency offset 50 ppm, carrier frequency 1 KHz and Doppler frequency $\mathrm{fd} = 6$ Hz. As a comparison, the classical frequency domain LS channel estimation approach [33] is simulated. To study the BER performance of DFE, the DFE which is regarded as individual module is embedded in the LS and proposed schemes. 18 received data points are averaged in DFE as described in (28). By comparing the curves 1, 2 with curves 3 and 4, we find that the proposed approach achieves much better BER performance than the LS algorithm. The improvement is more than 7 dB when SNR is higher than 15 dB. This is because proposed algorithm contains the fine estimation methods than can correct the phase rotation brought by the sample clock frequency offset and this can not be solved by the LS algorithm. In addition, the DFE also achieves 1 dB enhancement compared with the non-DFE structure according to the comparison between curve pairs curve 1–2 and curve 3–4.

Generally, compared with the frequency LS algorithm, the proposed algorithm can totally achieve more than 9 dB enhancement when SNR is higher than 15 dB.

Fig. 15 gives the decision-point SNR of the MMSE DFE in the condition of Rayleigh fading channel. For comparison, the SNR of Zero-forcing is derived as [29]:

$$SNRZF - DFE = \frac{1}{1 + \sum_i p_i^2} \bullet \frac{\varepsilon_x \bullet \|p\|^2}{N_0} \qquad (43)$$

This article has been accepted for publication in a future issue of this journal, but has not been fully edited. Content may change prior to final publication. Citation information: DOI10.1109/TBC.2012.2207249, IEEE Transactions on Broadcasting

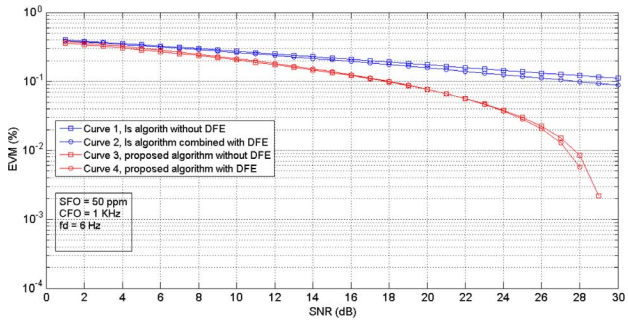

Fig. 14. BER vs. SNR for different algorithms in Rayleigh fading channel.

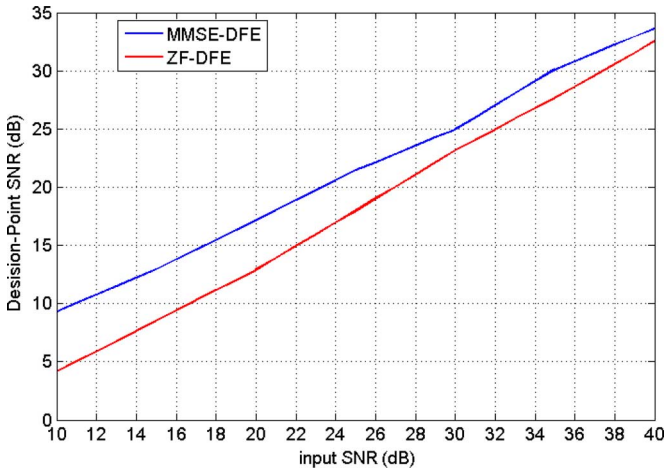

Fig. 15. Decision-point SNR of MMSE and ZF.

TABLE III
HARDWARE CONSUMPTION

	DSP48	Slice LUTs	Block RAM
Hardware Interface	0	959	12
Resampler	30	2274	6
Turbo Decoder	16	29877	69
DFE	12	1602	10
Entire Hardware resourse	769	150720	416

The SNR of ZF-DFE is also plotted. As expected, the proposed MMSE criterion results in a higher decision-point SNR than the ZF-DFE. It is 1 dB higher especially at low input SNR input SNR. This is because the average mechanism in the feedback filter can make use of the statistical information and eliminate the noise ingredients of input signal.

Table III shows the whole hardware consumption, which includes consumption of universal data interface, DFE module. And the consumption of turbo and viterbi decoder is also listed as a comparison. As can be seen from the table, the proposed MMSE DFE structure is easy to implement and consumes small hardware resources. The hardware interface consumes small part of the total hardware resource. And the rest of the hardware has plenty of resource provide powerful signal processing ability.

Table IV shows the general time consumptions for different average points. This simulation is carried out on the condition of $\mathrm{SFO} = 80\ \mathrm{ppm}$ and $\mathrm{CFO} = 1\ \mathrm{KHz}$ and all the algorithms are running on the MATLAB environment. As can be seen from the table, the preceding part of joint estimation algorithm which excluding DFE algorithm consume less than 10 minutes. However, the DFE consumes as much as 100 minutes when the average points are large. The DFE structure need more time to process more data points which indicates that it also consume more multiply-accumulate structure and RAM to store the data points. It reality, compromise between the estimation performance and resource consumption must be made.

TABLE IV
TIME CONSUMPTION FOR DIFFERENT AVERAGE POINTS

N	10	25	50	75	100	150	200	300
T(s)	9	16	28	38	46	68	87	132

VII. CONCLUSION

In this paper, a high-performance hybrid pilot-aided channel estimation scheme is proposed. This estimation algorithm first carries out a coarse frequency offset in time domain (TD) using training sequence to eliminate the dominant ICI caused by CFO. Furthermore, a low-complexity LS-based channel estimator is adopted to compensate for the imperfections of the channel. Then, frequency domain fine estimation with pilot-aided polynomial interpolation is formulated which reduce the residual CFO, SFO and CIR offset. In addition, a novel MMSE-based DFE scheme is introduced to enhance the EVM performance and this shows good performance at low SNR. The algorithm is verified via the FPGA-based co-simulation platform. The main contribution of this co-simulation is to propose a universal interface between MATLAB and FPGA which makes the most of high speed gigabit Ethernet and high performance FPGA to evaluate the proposed hybrid pilot-aided channel estimation for OFDM system. With little need for consideration of data transmission and hardware limitations, the developers can concentrate on the implementation, performance analysis and algorithm optimization. The simulation results based on this co-simulation platform has proven that the significant EVM performance improvement can be obtained by the proposed hybrid pilot-aided channel estimation in the large range of CFO, SFO and CIR, which is effective for OFDM systems.

REFERENCES

[1] M. Speth, S. A. Fechtel, G. Fock, and H. Meyr, "Optimum receiver design for wireless broad-band systems using OFDM.I.," *IEEE Trans. Communication*, vol. 47, no. 11, p. 1688-1677, Nov. 1999.

[2] H. Nguyen-Le, T. Le-Ngoc, and N. H Tran, "Iterative Receiver Design With Joint Doubly Selective Channel and CFO Estimation for Coded MIMO-OFDM Transmissions," *IEEE Trans. Vehicular Technology*, vol. 60, pp. 4052–4057, Oct. 2011.

[3] J. Li, G. Liu, and G. B. Giannakis, "Carrier frequency offset estimation for OFDM-based WLANs," *IEEE Signal Processing Letters*, vol. 8, pp. 80–82, Mar. 2001.

[4] D. Huang and K. B. Letaief, "Carrier frequency offset estimation for OFDM systems using subcarriers," *IEEE Trans. Communication*, vol. 54, pp. 813–823, May 2006.

[5] Z. Wensheng, L. Youming, Z. Xinxing, and Y. Jianding, "Blind Channel Estimation Algorithm with Simplified Implementation for OFDM System," *NSWCTC*, vol. 2, pp. 274–277, April 2010.

[6] S. Ghadrdan, M. Ahmadian, S. Salari, and M. Heydarzadeh, "An improved blind channel estimation algorithm for OFDM systems," in *IST 2009*, Dec. 2010, pp. 421–425.

[7] T. Hrycak, S. Das, G. Matz, and H. G. Feichtinger, "Practical Estimation of Rapidly Varying Channels for OFDM Systems," *IEEE Trans. Communication*, vol. 59, pp. 3040–3048, Nov. 2011.

This article has been accepted for publication in a future issue of this journal, but has not been fully edited. Content may change prior to final publication.
Citation information: DOI10.1109/TBC.2012.2207249, IEEE Transactions on Broadcasting

[8] S. Coleri, M. Ergen, A. Puri, and A. Bahai, "Channel estimation techniques based on pilot arrangement in OFDM systems," *IEEE Trans. Broadcasting*, vol. 59, pp. 223–229, Sep. 2002.
[9] Y.-H. Kim and J.-H. Lee, "Joint Maximum Likelihood Estimation of Carrier and Sampling Frequency Offsets for OFDM Systems," *IEEE Trans. Broadcasting*, vol. 57, pp. 277–283, Jun. 2011.
[10] M. Morelli and M. Moretti, "Fine carrier and sampling frequency synchronization in OFDM systems," *IEEE Trans. Wireless Communications*, vol. 9, pp. 1514–1524, Apr. 2010.
[11] S. U. H. Qureshi, *Adaptive Equalization*, vol. 73, pp. 1349–1387, June 2005.
[12] J. Proakis, *Digital Communications*, 3rd ed. Singapore: McGraw-Hill, 1995.
[13] S. Hayin, *Communication Syntems*, 3rd ed. New York: Wiley, 1994.
[14] N. Benvenuto and S. Tomasin, "on the comparison between OFDM and single carrier modulation with a DFE using a frequency-domain feedforward filter," *IEEE Trans. Communications*, vol. 60, June 2002.
[15] M. Ghogho and A. Swami, "Training Design for Multipath Channel and Frequency-Offset Estimation in MIMO Systems," *IEEE Trans. Signal Processing*, vol. 54, 2006.
[16] H. Nguyen-Le, T. Le-Ngoc, and C. C. Ko, "RLS-Based Joint Estimation and Tracking of Channel Response, Sampling, and Carrier Frequency Offset for OFDM," *IEEE Trans. Broadcasting*, vol. 55, no. 1, pp. 84–94, March 2009.
[17] E. Panayirci, H. Senol, and H. V. Poor, "Joint Channel Estimation, Equalization, and Data Detection for OFDM Systems in the Presence of Very High Mobility," *IEEE Trans. Signal Processing*, vol. 58, pp. 4225–4238, Aug. 2010.
[18] J.-J. van de Beek, O. Edfors, M. Sandell, S. K. Wilson, and P. O. Borjesson, *On Channel Estimation in OFDM Systems*, vol. 2, pp. 1090–3038, Jul. 1995.
[19] G. De Michell and R. Gupta, "Hardware/software co-design," *Proceeding of the IEEE*, vol. 85, pp. 349–365, Mar. 1997.
[20] S. Haykin, "Cognitive Radio: Brain-empowered Wireless Communications," *IEEE J. Sel. Areas Comm.*, vol. 23, no. 2, pp. 201–220, Feb. 2005.
[21] K. Amiri, Y. Sun, P. Murphy, C. Hunter, J. R. Cavallaro, and A. Sabharwal, "WARP, a Unified Wireless Network Testbed for Education and Research," in *IEEE Conference on Microelectronic Systems Education*, Jun. 2007, pp. 53–54.
[22] J. Heiskala and J. Terry, *OFDM Wireless LANs: A Theoretical and Practical Guide*. Indianapolis: Sams Publishing, December 2001.
[23] Y. Yao and G. B. Giannakis, *Blind Carrier Frequency Offset Estimation in SISO, MIMO, and Multiuser OFDM Systems*, vol. 52, p. 1832, Oct. 2004.
[24] R. Tesi, M. Hamalainen, and J. Iinatti, "Channel Estimation Algorithms Comparison for Multiband-OFDM," in *2006 IEEE 17th International Symposium on Personal, Indoor and Mobile Radio Communications*, Sep. 2006, pp. 1–5.
[25] B. Ai, Z.-X. Yang, C.-Y. Pan, J.-H. Ge, Y. Wang, and Z. Lu, "On the synchronization techniques for wireless OFDM systems," *IEEE Trans. Broadcasting*, vol. 52, no. 2, pp. 236–244, Jun. 2006.
[26] Y.-H. You, J. B. Kim, and H.-K. Song, "Pilot-Assisted Fine Frequency Synchronization for OFDM-Based DVB Receivers," *IEEE Trans. Broadcasting*, vol. 55, p. 674-648, Sep. 2009.
[27] *802 LAN/MAN Committee*, IEEE Std 802.11 -2009, Oct. 2009.
[28] M.-H. Hsieh and C.-H. Wei, "Channel estimation for OFDM systems based on comb-type pilot arrangement in frequency selective fading channels," *IEEE Trans. Consumer Electronics*, vol. 44, pp. 217–225, Feb. 1998.
[29] S. Diggavi, *Advanced Digital Communications*. Lausanne, Switzerland: EPFL, School of Computer and Communication Sciences, LICOS, Nov. 2005.
[30] R. Tesi, M. Hamalainen, and J. Iinatti, "Channel Estimation Algorithms Comparison for Multiband-OFDM," in *IEEE International Symposium on Indoor and Mobile Radio Communication*, Dec. 2006, pp. 1–5.

Wei Li received the B.Eng. from the University of Electronic and Science of Technology of China, in 2010.

He is currently working toward the Ph.D. degree at University of Bedfordshire, UK. He currently is involved in Aeroflex Ltd. UK for a project for the baseband signal process problem in LTE network. His research interests include signal processing for mobile communications, in cognitive radio, orthogonal frequency division multiplexing channel estimation, and cooperative communications via relays.

Yue Zhang (MIEEE, MIET) received his B.Eng. and M.Eng degree in 2001 and 2004 respectively at Beijing University of Post and Telecommunications. In 2008 he received his Ph.D. degree in Brunel University, UK.

He worked as a Research Engineer at Brunel University for the EU IST FP6 project- PLUTO. He is currently Senior Lecturer in the Department of Computer Science and Technology at the University of Bedfordshire on Royal Academy of Engineering Industrial Secondment with Aeroflex Ltd. in the high throughput wireless measurement platform project. He then worked as a Signal Processing Design Engineer in Anritsu. He was responsible for the RF/IF, digital and DSP design for various wireless communication systems. His research interests are signal processing, wireless communications systems, MIMO-OFDM systems, radio propagation model and multimedia and wireless networks.

Li-Ke Huang received his B.Sc. degree in electronic engineering at Shenzhen University China in 1998 and his Ph.D. degree in communication and signal processing at Imperial College London UK in 2003.

He is a technical expert and the Algorithms Group Leader at Aeroflex UK developing in test and measurement technologies for wireless system engineering. He specializes in transceiver algorithm and architecture designs for all major wireless communication standards. He is responsible for products and technologies research and development. His research interests are in communication system designs and signal processing algorithms and architectures.

Carsten Maple received his Ph.D. in Numerical Analysis from the University of Leicester in 1998, having completed a B.Sc. in Mathematics at the same institution.

He joined the University of Bedfordshire in the same year, was appointed to a personal chair in 2004 and became Head of the Department of Computer Science and Technology, a post he held until his appointment to Pro Vice Chancellor for Research and Enterprise in 2010. Carsten has published 150 papers in peer-reviewed journals and conference proceedings, been awarded millions of pounds in research grants through various national and international bodies, been a keynote speaker at a number of international conferences and has made numerous media appearances. His research interests are in distributed systems and communications.

He is a Fellow of British Computer Society and Head of the Information Group for the Council of Professors and Head of Computing, UK

John Cosmas is a Professor of Multimedia Systems in the School of Engineering and Design at Brunel University in West London. He co-leads the Wireless Networks and Communications Research Centre, (http://www.brunel.ac.uk/sed/ece/research/wncc), is the course director of M.Sc. Advanced Multimedia Design and 3D Technologies (http://www.brunel.ac.uk/sed/ece/courses/postgraduate/advanced-multimedia-design-and-3d-technologies-msc) and is an associate editor of IEEE TRANS. ON BROADCASTING. His research interests are concerned with the development of Multimedia Systems applied to Future of Broadcasting, the Future of Internet and 3D multimedia video/graphics design and the synergies between these technologies. He has participated in eleven EU-IST and two EPSRC funded research projects since 1986 and he has led three of these (CISMUNDUS, PLUTO, 3D MURALE).